DOI: 10.26461/27.06

Assessing the efficiency of bamboo biochar in microcystin-LR removal from water

Evaluación de la eficiencia del biochar de bambú en la eliminación de microcistina-LR del agua

Avaliação da eficiência do biochar de bambu na remoção de microcistina-LR da água

YANAÍNA CASTRO (1)
CAMILA HERNÁNDEZ (1)
ANA CLAUDIA PINA (1)(2)
DIANA MÍGUEZ (3)
MIRIAN ELIZABETH CASCO (1)
(1) Departamento de Ingeniería, Universidad Católica del Uruguay, Montevideo, Uruguay.
(2) Área de Fisicoquímica, Facultad de Química, Universidad de la República, Montevideo, Uruguay.
(3) Latitud - Fundación LATU, Montevideo, Uruguay.

RECIBIDO: 4/4/2024 → APROBADO: 30/5/2024 mirian.casco@ucu.edu.uy

ABSTRACT

Developing sustainable and cost-effective adsorbents for removing microcystin-LR (MCLR) is crucial. *Bambusa Tuldoides* was pyrolyzed at various temperatures (400, 500, and 600 °C) and residence times (0.5 and 2 h) to produce a series of biochars. The observed MCLR adsorption capacity (219 μg g^{-1} for 600B0.5 sample) under pH conditions similar to those in a water treatment plant (pH = 7.6) is mainly attributed to hydrophobic interactions, π-π stacking, and the basic nature of the biochars (pH_{PZC} > 8). A comprehensive analysis, including FTIR, elemental and proximate analysis, TG, SEM, N_2 adsorption, Hg porosimetry and Raman spectroscopy support this finding. Additionally, to compare 600B0.5 with commercially available activated carbon, a dynamic study was conducted using actual contaminated water. 600B0.5 sample exhibits a removal efficiency of 99.5 %, resulting in a final concentration of 0.28 μg L^{-1}, well below the World Health Organization guideline of 1 μg L^{-1}.
Keywords: biomass, pyrolysis, carbon, adsorption, cyanotoxin.

RESUMEN

Es fundamental desarrollar adsorbentes sostenibles y rentables para eliminar la microcistina-LR (MCLR). Se pirolizó *Bambusa Tuldoides* a varias temperaturas (400, 500 y 600 °C) y tiempos de residencia (0,5 y 2 h) para producir una serie de biochares. La

capacidad de adsorción de MCLR observada (219 µg g^{-1} para una muestra de 600B0.5) en condiciones de pH similares a las de una planta de tratamiento de agua (pH = 7.6) se atribuye principalmente a las interacciones hidrofóbicas, al apilamiento π-π y a la naturaleza básica de los biochares (pH_{PZC} > 8). Un análisis exhaustivo, que incluye FTIR, análisis elemental y próximo, TG, SEM, adsorción de N_2, porosimetría de Hg y espectroscopia Raman, respalda este hallazgo. Además, para comparar el 600B0.5 con un carbón activado disponible comercialmente, se realizó un estudio dinámico utilizando agua contaminada real. La muestra 600B0.5 exhibe una eficiencia de eliminación del 99,5 %, lo que da como resultado una concentración final de 0.28 µg L^{-1}, muy por debajo del valor de referencia de la Organización Mundial de la Salud de 1 µg L^{-1}.
Palabras clave: biomasa, pirólisis, carbón, adsorción, cianotoxina.

RESUMO

É essencial desenvolver adsorventes sustentáveis e econômicos para remover a microcistina-LR (MCLR). *Bambusa Tuldoides* foi pirolisado em temperaturas variadas (400, 500 e 600 °C) e tempos de residência (0,5 e 2 h) para produzir uma série de biochares. A capacidade de adsorção de MCLR observada (219 µg g^{-1} para uma amostra de 600B0.5) em condições de pH semelhantes às de uma planta de tratamento de água (pH = 7,6) é atribuída principalmente às interações hidrofóbicas, o apilamiento π-π e a naturalidade básica do biochar (pH_{PZC} > 8). Uma análise exaustiva, que inclui FTIR, análise elementar e imediata, TG, SEM, adsorção de N_2, porosimetria de Hg e espectroscopia Raman apoia esta descoberta. Além disso, para comparar o 600B0.5 com um carvão ativado disponível comercialmente, foi realizado um estudo dinâmico utilizando água contaminada real. A mostra 600B0.5 apresenta uma eficiência de remoção de 99,5 %, resultando em uma concentração final de 0.28 µg L^{-1}, bem abaixo do valor de referência da Organização Mundial da Saúde de 1 µg L^{-1}.
Palavras-chave: biomassa, pirólise, carvão, adsorção, cianotoxina.

INTRODUCTION

Cyanobacterial blooms, caused by water eutrophication, have increased worldwide, posing risks to humans, animals, and plants due to the production of cyanotoxins. At a global scale, cyanotoxins have been found responsible for illness and death of wild and domestic animals (aquatic and terrestrial) and human health issues ranging from contact irritations and gastrointestinal distress to acute, chronic, and lethal poisonings (Carmichael y Boyer, 2016).

Microcystins (MCs) are potent toxins that *Microcystis aeruginosa* and other cyanobacteria produce. They are one of the most prevalent and harmful cyanotoxins groups, and their presence in water bodies poses a significant risk to both humans and animals. In particular, microcystin-LR (MCLR) are hepatotoxic peptides that inhibit protein phosphatases, induce DNA damage and mutations in mammalian cells, disrupt the

mitotic spindle, and promote genetic instability, gene expression changes, and cell death, leading to potential carcinogenic activities (Zegura, 2016).

There is a growing concern about the presence of MCLR in freshwater sources, such as lakes, reservoirs, and rivers, as well as in drinking water supplies, posing threats to aquatic and terrestrial plants and agricultural soils used for crop production. Studies have indicated potential health risks associated with contaminated fruits and vegetables sourced from irrigated water containing MCs (Melaram et al., 2022). Furthermore, MCLR can accumulate in aquatic organisms like fish and shellfish, leading to its bioaccumulation in the food chain.

Cyanobacterial's toxins are highly stable and widely distributed hepatotoxins that can accumulate and transfer to higher trophic levels. The human health risks from MCs involve consistent low-level exposure through various channels like physical contact, drinking contaminated water, consuming tainted food, and hemodialysis. Drinking contaminated water and eating affected food are the primary exposure routes. Investigating the migration and transmission of MCs is crucial to reduce human exposure (Ren et al., 2023). The World Health Organization recommends a guideline level of 1 μg L^{-1} for microcystin-LR in drinking water to ensure the protection of human health (World Health Organization, 2020).

Ensuring complete removal of the toxin from water sources is a complex challenge. Traditional water treatment methods, such as conventional coagulation, sedimentation, filtration, and disinfection, are ineffective in eliminating MCLR (Verma et al., 2023). El Bouaidi et al. (2022) reviewed the use of various adsorbents used for MCs removal from water sources, considering that activated carbon constitutes the most widely used adsorbent for treating contaminated waters. In the case of Uruguay, the most recent tender resulted in the procurement of 600 tons of activated carbon for use in the drinking water treatment process (Uruguay. Agencia Reguladora de Compras Estatales, 2022). This purchase was imported at a cost of USD 762,348.00, approximately USD 1,270.58 per ton.

As current remediation methods require more environmentally friendly and cost-effective adsorbents, biochar has lately gained attention with its high porosity and sorption efficiency. Pyrolysis was evaluated as a method to produce efficient adsorbents for MCs removal, highlighting its cost-effectiveness, but its potential depends on feedstock and pyrolysis conditions (Frišták et al., 2020).

Bamboo as a raw material is a good choice as it has high biomass production and a rapid ripening period. Additionally, it is easy to manage in cultivation, renewable, non-toxic, and biodegradable. Bamboo-derived biochars provide an environmentally friendly, cost-effective, and technologically feasible solution removing pollutants to improve drinking water quality. Particularly, bamboo biochars exhibit unique structural and surface properties when compared to activated carbon (Li et al., 2018).

Pollutant removal mechanisms involved electrostatic attraction, pore-filling, hydrogen- bonding effect and π-π electron donor-acceptor interaction, but predominant mechanisms varied for different biochars (Li et al., 2018). The mechanism that influences the adsorption capacity of MCLR on biochars remains a subject of ongoing debate in the literature. The polarity, hydrophilicity/hydrophobicity, and the aromatization degree of the biochar affects the MCs adsorption performance.

For instance, Li et al. (2018) reported π ± π electron-donor-acceptor interactions dominate in the adsorption of MCLR on biochar (from plant- and animal-wastes) produced at 600 °C, in contrast to those produced at 300 °C. While Li et al. (2014) proposed that the adsorption mechanisms may be primarily associated with the Coulombic attractions and the hydrogen bond interactions between MCLR and the surface of biochars obtained at 300 °C. The statement that only one specific interaction between biochars and MCLR maximizes removal capabilities is inaccurate, as more than one mechanism can be involved, and the characteristics of the starting biomass material must also be considered.

Therefore, the central objective of this study is to assess the physical-chemical properties of bamboo biochar, elucidating possible mechanisms of adsorption that improve the removal of MCLR from aqueous solutions, thus advancing towards the adoption of bamboo biochar in water treatment processes.

MATERIALS AND METHODS

Preparation of bamboo biochars

Three-year-old wild *Bambusa Tuldoides* were supplied by the company Bambú del Este to produce biochar. The bamboo culms were oven-dried at 105 °C for 24 h and then chipped and passed through to 120 mesh sieves (120 µm). Pyrolysis of prepared biomass was carried out in a tubular furnace (Snol LXC04) under a nitrogen atmosphere (purity > 99.9 % Air Liquid, N50) with a heating rate program 5 °C min^{-1} up to the predetermined temperatures of 400 °C, 500 °C, 600 °C and residence time of 0.5 and 2 h. The bamboo biochars produced at different combination temperature and time were named 400B0.5, 400B2.0, 500B0.5, 500B2.0, 600B0.5, and 600B2.0, where the prefix and suffix numbers stand for the pyrolysis temperature (°C) and the time (hour), respectively.

Bamboo and bamboo biochars characterization

The carbon (C), hydrogen (H), nitrogen (N), and sulfur (S) contents were determined using an Elemental Analytical Instrument (Thermo Scientific Flash 2000 Organic Elemental Analyzer CHNS0). The oxygen (O) contents were calculated by difference according to mass balance.

The bamboo and bamboo biochars were analyzed for moisture, volatile matter (VM), fixed carbon (FC) and ash content (Ash). Moisture was calculated by weight difference between the sample before and after being exposed at 105 °C in an oven until constant weight. The VM and Ash were tested according to the protocol (American Society for Testing and Materials, 2021). The FC was calculated on dry basis by difference according to mass balance.

Thermogravimetric analysis (TG) was performed using a SDT Q600 thermal analyzer (TA instrument) at heating rates of 10 °C min^{-1} with temperatures ranging from room temperature to 900 °C. Compressed air and nitrogen was used for combustion experiments at 50 mL min^{-1}. About 5 ± 0.2 mg sample was weighed and placed in a platinum crucible.

Surface morphologies were observed by scanning electron microscopy (JEOL JSM- 5900LV equipment under 20 kV of the voltage) after sputtering with gold.

The point of zero charge (pH_{PZC}) of the bamboo biochars was measured by the drift method, where 0.5 g of the biochar powdered sample were added to the pH-adjusted solution (3, 4, 5, 6, 8, 10, 11) in a Erlenmeyer flask, capped and placed in the shaker. Then, the final pH of the solutions was measured after 48 hours at room temperature with a HANNA Instruments HI 2211 pH-meter and the ΔpH (difference between initial pH and final pH) against the initial pH was plotted, in which the value of pH_{PZC} was found where the ΔpH = 0.

Surface functional groups were determined by Fourier transform infrared spectroscopy analysis (FTIR) via a FTIR spectrometer Shimadzu IRSpirit-T (KBr window), QATR-S (wide-band diamond crystal). The spectra were recorded at a resolution of 4 cm^{-1} through wavelength scanning range of 4000–400 cm^{-1}.

Confocal Raman imaging was applied to all the samples using a WITec equipment, Alpha 300RA model. Raman spectra were collected utilizing a 532 nm (2.33 eV) excitation wavelength. Representative spectra were collected using 100 accumulations of 0.5 seconds per spectrum.

The nitrogen adsorption/desorption isotherms were measured at -196 °C using an ASAP2000 equipment (Micromeritics). Before any physisorption measurements, the samples were degassed for 12 h at 150 °C. The carbons' apparents specific surface area (S_{BET}) was calculated using Brunauer-Emmett-Teller (BET) equation in the range that fits the consistency criteria proposed by Rouquerol et al. (2007). The total pore volume (V_t) was calculated at a relative pressure 0.95 according to the Gurvich rule. Micropore volume (V_{micro}) was calculated by applying Dubinin-Raduschevich equation. The difference between V_t and V_{micro} is considered as V_{meso}.

Mercury intrusion-extrusion porosimetry was measured from 0.002 up to 150 MPa on porosimeter analyzer AUTOPORE III 9410 (Micromeritics). The samples (bamboo and bamboo biochars in powder) were previously degassed to a residual pressure of 30 μmHg. Specifc surface area (S_{Hg}), total pore volume ($V_{TP\text{-}Hg}$), porosity percentage, and pore size distribution were obtained from mercury intrusion data.

Microcystin-LR (MCLR) adsorption studies

The removal efficiency (E) of an adsorbent on MCLR is defined as:

$$E = \frac{(C_0 - C_e)}{C_0} \cdot 100\ \% \qquad (1)$$

Where, C_0 (μg L^{-1}) is the initial concentration and C_e (μg L^{-1}) is the equilibrium concentration of MCLR.

Kinetic experiments were conducted with 500 μg L^{-1} of MCLR (Eurofins Abraxis, standar 0.5 mg) and 0.1 g L^{-1} of adsorbent 600B0.5 mixing in Erlenmeyer flasks using 30 mL of solution. Samples were taken out at different predetermined time (5, 15, 30, 60, 120, 300, 1440 min) to evaluate the residual MCLR concentrations. Similarly, equilibrium isotherm sorption

experiments were conducted using various initial concentrations of MCLR (20, 150, 350, 500 μg L^{-1}) mixed with a dose of 6.0 g L^{-1} of the bamboo biochar 600B0.5. All the experiments were conducted in Erlenmeyer flasks using 30 mL of solution. The equilibrium time was set as 24h. MCLR concentration was determined with a high-performance liquid chromatograph (HPLC) Separation Module 2695 (Water Alliance, detector Photodiode array 2998).

The adsorption amount (Q_e) was calculated according to equation:

$$Q_e = \frac{(C_0 - C_e)}{m} \cdot V \quad (2)$$

Where, C_0 (μg L^{-1}) is the initial concentration and C_e (μg L^{-1}) is the equilibrium concentration of MCLR; m is the weight of biochar (g), and V is the solution volume (L).

Lagmuir model were used to fit the adsorption isotherms according to the equation:

$$Q_e = \frac{Q_{max} \cdot K_L \cdot C_e}{1 + K_L \cdot C_e} \quad (3)$$

Where K_L (L μg^{-1}) is the Langmuir adsorption coefficient, and Q_{max} (μg g^{-1}) is the saturated adsorption capacity.

Freundlich model were used to fit the adsorption isotherms according to the equation:

$$Q_e = K_F \cdot C_e^{\,n} \quad (4)$$

Where K_F (μg^{1-n} L^n g^{-1}) is the adsorption coefficient, and n is the Freundlich constant describing the nonlinearity of isotherms, and is related to the surface site heterogeneity of the sorbent.

The pseudo-first order equation and pseudo-second order equation models were used to adjust the experimental data in this study. The kinetics equation models are the follow:

Pseudo-first order:

$$Q_t = Q_e \cdot (1 - e^{-K_1 t}) \quad (5)$$

Pseudo-second order:

$$Q_t = \frac{k_2 \cdot Q_e^2 \cdot t}{(1 + K_2 \cdot Q_e \cdot t)} \quad (6)$$

Where Q_e and Q_t (μg g^{-1}) are the amounts of MCLR adsorbed at equilibrium and at a time, t, respectively. K_1 and K_2 are the rate constants for pseudo-first-order and pseudo-second-order kinetics, respectively.

RESULTS AND DISCUSSION

Characterization of bamboo biochars

A series of six bamboo biochars were produced by pyrolyzing three-year-old wild *Bambusa Tuldoides* (referred to as 'bamboo' hereafter) at varying temperatures (400, 500, and 600 °C) and residence time (0.5 and 2 hours). A fibrous biomass like bamboo consists of cellulose, hemicelluloses, and lignin with smaller quantities of organic extractives and inorganic minerals (Chaturvedi et al., 2023). Notably, an inverse relationship is observed between the pyrolysis temperature and the yield of each biochar, attributed to the detachment of volatile matter. At the same time, carbon fixation occurs during carbonization (Table 1). This trend is less marked when keeping the temperature but varying the residence time.

Thermogravimetric analyses conducted in nitrogen atmospheres (refer to Figure A1) corroborate these tendencies. The weight loss pattern of bamboo in a nitrogen atmosphere exhibits a significant reduction in mass within the temperature range of 200–300 °C, corresponding to the release of volatile matter coming, first from the decomposition of extractive and, then from the decomposition of hemicellulose (Manals-Cutiño et al., 2011). Between 300 and 600 °C, the gradual decrease is consistent with the biochar yields related to various pyrolysis temperatures (Table 1), corresponding to cellulose decomposition (Manals-Cutiño et al., 2011).

TABLE 1. Yields, proximate analysis (on a dry basis), elemental compositions and atomic ratios on an ash-free basis for bamboo and the six bamboo biochars.

Sample	Yield[a] (%)	Ash (wt. %)	VM (wt. %)	FC[b] (wt. %)	C (at. %)	H (at. %)	N (at. %)	S (at. %)	O (at. %)	(N+O)/C[c]	H/C[d]	O/C[e]
Bamboo	-	8.1	79.2	12.7	35.6	44.1	0.3	0.0	20.0	0.57	1.24	0.56
400B0.5	37.9	6.1	30.0	63.9	59.6	30.7	0.5	0.1	9.1	0.16	0.51	0.15
400B2.0	37.4	6.2	27.8	66.0	62.4	30.5	0.5	0.1	6.6	0.11	0.49	0.11
500B0.5	33.0	6.2	26.7	67.1	67.8	26.7	0.6	0.1	4.8	0.08	0.39	0.07
500B2.0	32.4	6.4	16.1	77.5	71.5	24.3	0.6	0.1	3.5	0.06	0.34	0.05
600B0.5	30.7	5.2	10.2	89.6	76.2	18.3	0.6	0.1	4.7	0.07	0.24	0.06
600B2.0	30.8	5.8	9.9	84.3	79.7	16.5	0.5	0.2	3.2	0.05	0.21	0.04

[a] Yield (%) = (weight of bamboo biochar) / (weight bamboo) x 100, [b] FC (%) = 100 - ash (%) -VM (%), [c] (N + O)/C: atomic ratio of the sum of nitrogen and oxygen to carbon, [d] H/C: atomic ratio of hydrogen to carbon, [e] O/C: atomic ratio of oxygen to carbon.

From the scanning electron microscopy images obtained (refer to Figure A2), it can be observed that the bamboo, before carbonization, exhibited organized and well-oriented fibers, forming a structural unit. On the other hand, in the images of the biochar 500B2.0, small independent domains of carbon fibers are randomly distributed. This can be

associated with the bamboo decomposition mechanism during the pyrolysis process. In the thermogravimetric study conducted on bamboo, characteristic temperatures of the thermal decomposition process of biomass were identified, and the regions where different mass losses are experienced were established. At 500 °C, hemicellulose and cellulose had already decomposed. As the micro-fibrils of cellulose, which form the matrix where lignin and hemicellulose intertwine, degrade, the bamboo loses its structure, a result that can be observed in the images of the biochar obtained after carbonization at 500 °C.

Elemental analysis results indicate that increasing the pyrolysis temperature leads to an increment in the carbon (C) content while diminished the levels of oxygen (O) and hydrogen (H). The decreasing atomic ratios of H/C and O/C suggest the aromatization of biomass, a phenomenon later confirmed by Raman analysis. The diminishing polarity index ((O+N)/C) indicates a decrease in surface polar functional groups. According to the literature, these ratios indicate biochar's hydrophobic/hydrophilic nature (Chen y Chen, 2009). Consequently, for the bamboo biochars in this study, a concurrent reduction in hydrophilicity accompanies the rise in pyrolysis temperature. In other words, the gradual elimination of oxygen (and nitrogen)-containing groups from the biomass results in a more hydrophobic biochar framework. As anticipated in previous research in the literature (Teng et al., 2013a), this property promotes hydrophobic interactions between the surface of biochars and the hydrophobic moieties of MCLR (leucine).

Confocal Raman microscopy was utilized to assess the amorphization/aromatization process of bamboo biochar under varying temperature and time treatments. Raman spectra in Figure 1a, indicate an excellent homogeneity in the carbonaceous signals, corresponding to G and D bands along all the analyzed samples (refer to Table A1). All the signals plotted correspond to that of amorphous materials (Fries y Steele, 2010). However, recorded data show a graphitic increment, especially with temperature treatment (I_G increment), leading to an increment in the structure's order according to the I_D/I_G contribution results.

In line with elemental analysis, this indicates that as the temperature increases the aromatic carbon frameworks gradually develop, offering additional binding sites via π-π stacking interaction between the aromatic units and the benzene ring of MCLR (Teng et al., 2013b).

Figure 1b portrays the FTIR spectra for all the bamboo biochars. Biochars are complex materials with several distinctive functional groups, and the FTIR results concord with those previously reported (Odoemelam et al., 2015). The characteristic signal recorded at 750 cm^{-1} is assigned to =C-H bending out of plane vibration, while 800 and 880 cm^{-1} are assigned to =C-H ring torsion and C-H bending and ring puckering, respectively. The presence of alcohols and, or phenols is confirmed by the 1110 and 1373 cm^{-1} vibrating bands, corresponding to C-O stretching and O-H bending. The signal at 1574 cm^{-1} assigned to C=C stretching is recorded for all the samples. The signal that showed a more extensive signal modification depending on the treatment (not only the temperature but also the time of treatment as can be seen for 500 samples series) is assigned to C=O (bonded with H) stretching associated with carboxylic acids and derivatives groups located at 1700 cm^{-1}.

The point of zero charge (pH_{PZC}) was measured to further analyze the physical-chemical properties of the bamboo biochar's surface (Figure A3). The pH_{PZC} value gradually

improved with pyrolysis temperature. It ranges from 7.92 to 8.66 from 400B0.5 to 600B2.0, respectively (Table 2). Since $pH_{PZC} > 7$, all obtained bamboo biochars are basic in nature. This behavior is in line with the FTIR functional group analysis, which confirms the reduction of carboxylic acid content with increasing temperature. The pH_{PZC} represents the solution pH at which the surface charge of biochar becomes neutral, which means biochar may exhibit a negative charge at $pH > pH_{PZC}$ and a positive charge at $pH < pH_{PZC}$.

TABLE 2. Textural properties and zero-point charge (pH_{PZC}) of the six bamboo biochars.

Sample	S_{BET} (m^2/g)	V_{micro} (cm^3/g)	V_t (cm^3/g)	V_{meso} (cm^3/g)	S_{Hg} (m^2/g)	$V_{t,Hg}$ (cm^3/g)	Porosity (%)	ρ_{bulk} (g/cm^3)	$\rho_{skeletal}$ (g/cm^3)	pH_{PZC} (%)
400B0.5	2	0.001	0.001	0.000	23.8	1.47	60.1	0.41	1,02	7.92
400B2.0	2	0.001	0.002	0.001	23.7	1.54	60.1	0.39	0,98	7.97
500B0.5	3	0.001	0.002	0.001	24.6	1.05	49.5	0.47	0,93	8.42
500B2.0	8	0.003	0.005	0.002	22.9	1.18	51.2	0.43	0,89	8.52
600B0.5	64	0.027	0.027	0.000	20.7	1.33	55.8	0.42	0,95	8.66
600B2.0	67	0.029	0.029	0.000	16.3	1.53	58.4	0.38	0,91	8.66

When MCs are present in the water before entering the purification plant, the pH typically ranges between 7 and 7.9 (Uruguay. Ministerio de Vivienda, Ordenamiento Territorial y Medio Ambiente, 2020), which means that the biochar surface will be positively charged under this condition. At this point, it is crucial to consider the MCLR molecule's nature and its features. The ionizable entities in MCLR, which consist of two carboxyl groups and one guanidino group, can undergo deprotonation or protonation, resulting in a positively or negatively charged MCLR at varying pH. As indicated by the pKa values of MCLR (pKa1, 2.09; pKa2, 2.19; pKa3, 12.48), when the solution pH is neutral (or slightly basic), MCLR predominantly exists in the form of anion $MCLR^-$ (Li et al., 2014).

Therefore, at the pH typically found in water treatment plants, the adsorption of MCLR onto bamboo biochars is likely to be enhanced by electrostatic attraction between the positively charged biochar surfaces and the negatively charged MCLR.

The textural properties of adsorbent materials significantly influence the adsorption process. Figure 1c displays the nitrogen adsorption/desorption isotherms of the six biochars. According to the IUPAC classification, all samples exhibit a Type I isotherm (Thommes et al., 2015), indicating their character as microporous adsorbent materials. The specific surface area (S_{BET}), the total pore volume (V_t), and the micropore volume (V_{micro}), were determined to further analyze the adsorption performance of bamboo biochars. Even though increasing pyrolysis temperatures enhances these values (Table 2), the most significant increase observed at 500 °C for 2.0 hours and 600 °C for 0.5 hours, where the specific surface area (S_{BET}) increases from 8 to 64 $m^2\ g^{-1}$, respectively. According to the isotherm shape (type I), all the bamboo biochars still exhibit micropores (pore diameters less than 2 nm). The three-dimensional size of the MCLR molecule was documented as 1.9 nmx1.5 nmx1.1 nm, with the maximum length and second-widest dimension of 2.94 nm and 2.55 nm, respectively (Teng et al., 2013b), falling in the lower

limit of mesopore size range (2-50 nm), it is expected that steric hindrances hinder the diffusion of the microcystin molecule into those micropores, potentially making it less effective in the removal process.

Hence, the presence of substantial mesopores or macropores within the bamboo biochars was characterized through Hg porosimetry. The corresponding mercury intrusion-extrusion curves can be found in Figure A4. Notably, all bamboo biochars display a considerable increase in accumulated volume at low pressures, specifically at 0.2 MPa, signifying the presence of large macropores exceeding 1 µm in diameter. Figure 1d presents the pore size distribution (PSD) data obtained from Hg porosimetry, revealing an average pore diameter of 11 µm. This pore size does not obstruct water flow, potentially leading to improved MCLR diffusion into the interior of the particle, thus enhancing the adsorption kinetics (as we will discuss later). A summary of the textural properties obtained from the mercury porosimetry data is provided in Table 2.

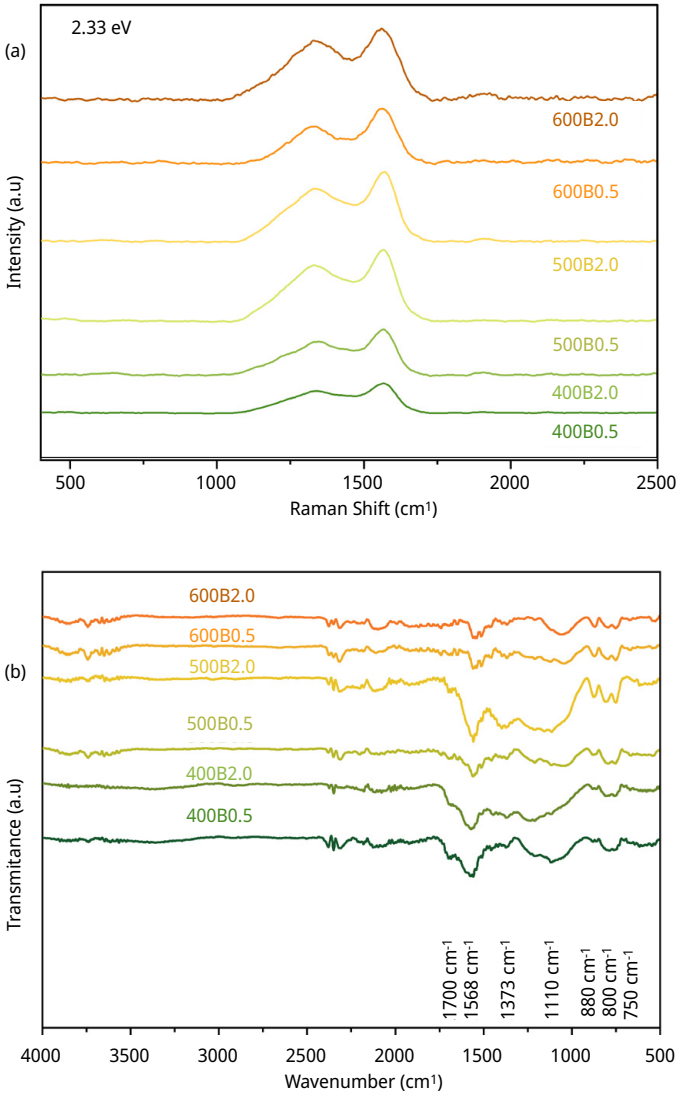

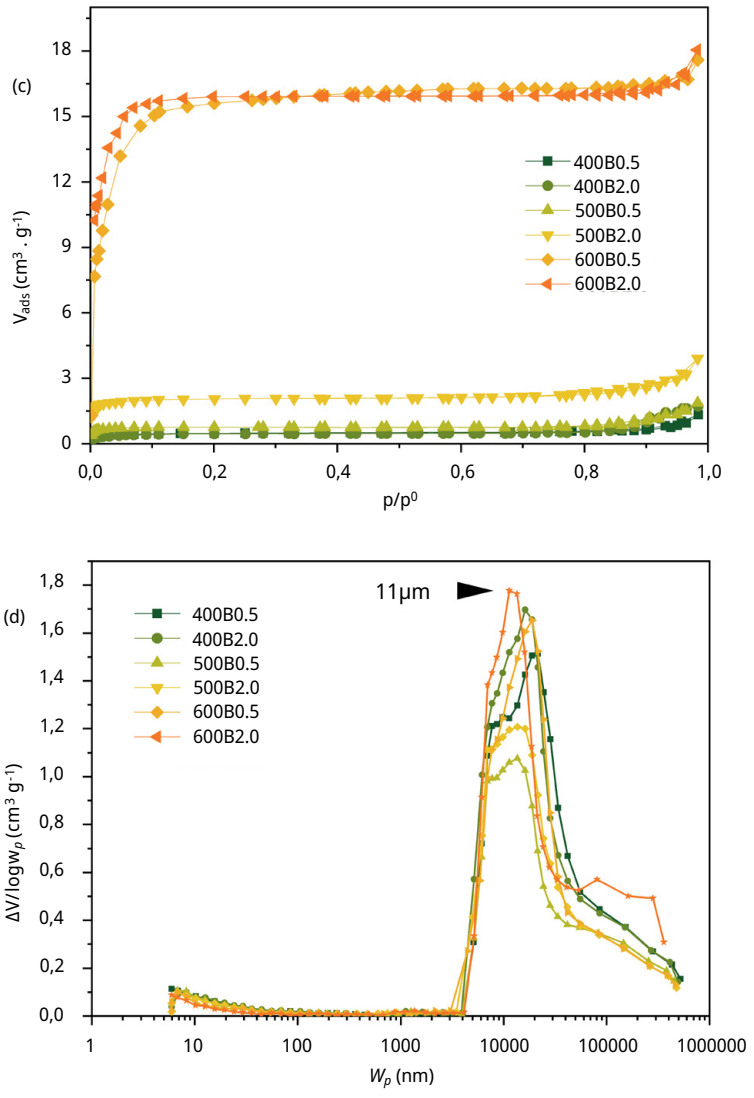

FIGURE 1. Surface and textural characterization of the six bamboo biochars. (a) Raman spectra of the six bamboo biochars, (b) FT-IR spectra, (c) N_2 adsorption/desorption isotherms and (d) pore size distribution obtained from Hg intrusion data.

MCLR adsorption performance

Initially, we calculated the MCLR removal efficiency (%) of all biochars at different initial concentrations (C_0 = 20 (18.1), 150 (153), 350 (370), 500 (525) µg L^{-1}). All samples showed excellent removal efficiency percentage (> 86.7 %) when the initial concentration was relatively low (Figure 2). The main differences can be observed at the maximal concentration of MCLR 500 (525) µg/L. In this case, the removal efficiency was 53.9 % and 61.3 % for 400B0.5 and 400B2.0, respectively. Conversely, the remaining bamboo biochars demonstrated a significantly higher removal efficiency, exceeding 91 %. The removal

efficiency, the adsorption isotherms (Figure A5), and the Langmuir and Freundlich fitting parameters are listed in Table 3.

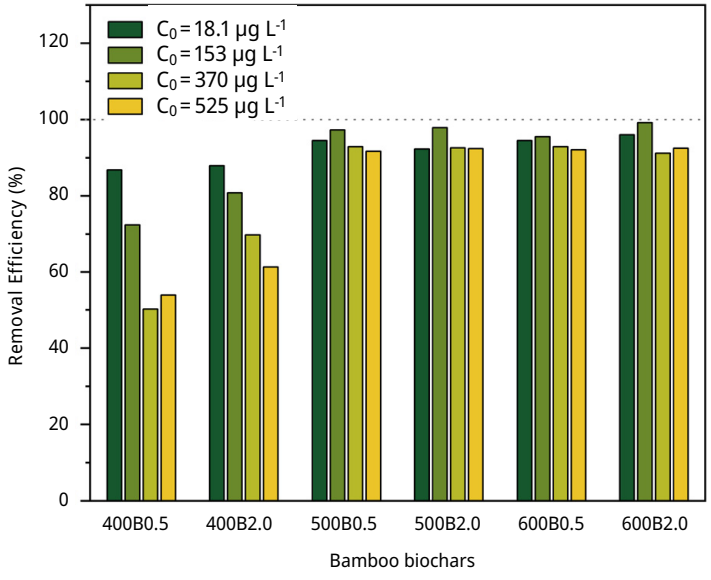

FIGURE 2. MCLR adsorption performance. Removal efficiency (%) of the six bamboo biochars in batch.

The superior performance of bamboo biochars obtained at pyrolysis temperatures of 500 and 600 °C can be attributed to their pH_{PZC}. The pH of the initial solution was 7.63, aligning with the typical pH conditions encountered in water treatment plants. Then, the significance of a pH_{PZC} exceeding 8 becomes evident in enhancing the MCLR removal capacity of bamboo biochars via electrostatic attraction between the positively charged bamboo biochar surfaces and the negatively charged MCLR. These findings present a significant advantage for applying bamboo biochars as adsorbents, as there is no need to adjust the pH to ensure their optimal performance.

TABLE 3. Langmuir and Freundlich fitting parameters of MCLR adsorption isotherm, and removal efficiency (%) calculated in for a concentration of MCLR of 525 µg/L (adsorbent dose 6 g/L).

Sample	Langmuir model			Freundlich model			
	K_L (L g^{-1})	Q_{max} (µg g^{-1})	R_{adj}^2	K_F (µ$g^{1-n}L^n g^{-1}$)	n	R_{adj}^2	Removal Efficiency (%)
400B0.5	0.007	46.605	0.9514	1.284	0.575	0.9765	53.9
400B2.0	0.0127	61.685	0.9816	2.856	0.523	0.9363	61.3
500B0.5	0.033	106.29	0.9825	5.551	0.523	0.9872	81.2
500B2.0	0.0843	73.170	0.9083	7.433	0.523	0.9185	92.4
600B0.5	0.0113	218.95	0.9640	4.569	0.733	0.9958	92.1
600B2.0	0.2393	69.600	0.8342	12.088	0.459	0.8513	92.5

Considering the characterization of bamboo biochars and removal efficiency results, we have identified sample 600B0.5 as a potential candidate to replace activated carbon in a hypothetical water treatment plant. Among the bamboo biochars exhibiting a removal efficiency exceeding 91 %, sample 600B0.5 (pH_{PZC} = 8.66) stands out due to its relatively elevated specific surface area (S_{BET} = 64 m^2 g^{-1}) and high graphitization degree (indicated by the lowest I_D/I_G ratio, 2.08), combined with a shorter residence time (0.5 h). The maximum adsorption capacity (Q_{max}) obtained through Langmuir fitting was 219 µg g^{-1} for this sample.

The adsorption kinetics of MCLR on the selected bamboo biochar (600B0.5) reveals a rapid increase in the adsorption capacity of MCLR within the initial 20 min, signifying a fast adsorption process. In contrast, the adsorption equilibrium is reached at approximately 2-3 h (refer to Figure A6). The exceptional kinetic properties can be attributed to the macroporous structure of the bamboo biochar, as evidenced by Hg porosimetry, allowing an easy path to reach the adsorption sites. Furthermore, the saturation adsorption amount obtained by fitting the pseudo-second-order kinetic model is 262 µg g^{-1}, which closely aligns with the experimental equilibrium adsorption capacity of 600B0.5 (200 µg g^{-1}) and the Langmuir equation fitting. This model is usually applied when chemisorption controls the adsorption kinetic.

Powdered activated carbon (PAC) and granular activated carbon (GAC) are frequently employed in water treatment plants to eliminate undesirable taste, odor, and various organic compounds, including MCs, through the adsorption process. In this context, we conducted a column experiment to evaluate the dynamic adsorption behavior of the selected bamboo biochar (600B0.5) compared to a commercially available activated carbon (AC) toward removing MCLR in a complex matrix.

A photograph of the experimental set-up is provided in Figure A7. The contaminated water from a real water source, supplied by the National Administration of State Sanitary Works (OSE), a state-owned Uruguayan Water Utilities company, was introduced into the column at a flow rate of 8 mL min^{-1}. The supplied source water underwent standard water treatment processes, including coagulation, flocculation and sedimentation in the plant. No filtration process was applied. The conventional treatments proved ineffective in removing extracellular/dissolved cyanotoxins (Verma et al., 2023). Therefore, we deliberately introduced 58 µg L^{-1} of MCLR into this sample to simulate an extreme scenario of cyanobacteria blooms.

After passing through the column, the resulting solution contains less than 1 µg L^{-1} of MCLR for both adsorbents (0.28 µg L^{-1} for 600B0.5 and 0.52 µg L^{-1} for the AC), falling below the recommended guideline level for drinking water (World Health Organization, 2020). This is a removal efficiency of 99.5 % for 600B0.5 and 99.1 % for the AC. Results are promising for two reasons: firstly, other organic compounds or minerals in the water could interfere with the adsorption process. However, both adsorbents demonstrate resilience to such interferences, maintaining their effectiveness. Secondly, in comparing activated carbon with bamboo biochar, the latter possesses a significantly lower surface area (64 m^2 g^{-1} vs. 1000 m^2 g^{-1}), as it does not undergo an activation process, rendering the bamboo biochar a comparatively more cost-effective adsorbent.

Discussion of the adsorption mechanism on bamboo biochars

The adsorption mechanisms of MCLR on carbonaceous materials, such as porous carbon and biochars, are determined by their surface chemistry and textural characteristics. MCLR is a large and complex molecule that interacts with sorbents through hydrophobic forces, electrostatic attraction, pore-filling, hydrogen bond, and π-π interaction (Frišták et al., 2020; Pendleton et al., 2001).

Under the pH condition comparable to the incoming water at the water treatment plant, the bamboo biochar pyrolyzed at 600 °C for 0.5 hours (600B0.5) achieved the highest MCLR removal efficiency. This pyrolysis temperature renders a biochar with 1) a hydrophobic surface promoting hydrophobic interaction with the leucine moieties of MCLR, 2) a high aromatization degree of the carbonaceous structure, promoting a π-π stacking with the benzene group of MCLR, and 3) a basic nature (pH_{PZC} > 8), promoting electrostatic attractions with the anion $MCLR^-$. The chemical structure of MCLR is presented in Figure A8 and the proposed mechanisms are schematized in Figure 3. Although the pores are essentially small to adsorb MCLR, bamboo biochars exhibit a highly developed macroporosity that accelerates the diffusion of pollutants toward the surface of the biochars.

In summary, bamboo biochars emerge as a promising candidate for effectively removing MCLR from real water sources. The adsorption capacity rivals and even surpasses other adsorbents such as wood-based activated carbon (Pendleton et al., 2001) and rice straw-derived biochar (Wei and Lu, 2021). Upon comparison with diverse carbonaceous materials outlined in Table 4, bamboo biochars exhibit several advantageous qualities. Using bamboo biomass as a sustainable starting material, free from chemicals associated with an activation process, suggests potential benefits for sustainability and reduced environmental impact. The effective performance of bamboo biochars at the studied pH eliminates the necessity for pH adjustment when utilized in a water treatment plant. When comparing different carbonaceous materials, it is crucial to consider production costs, giving special attention to biomass residues that have the potential to compete with bamboo.

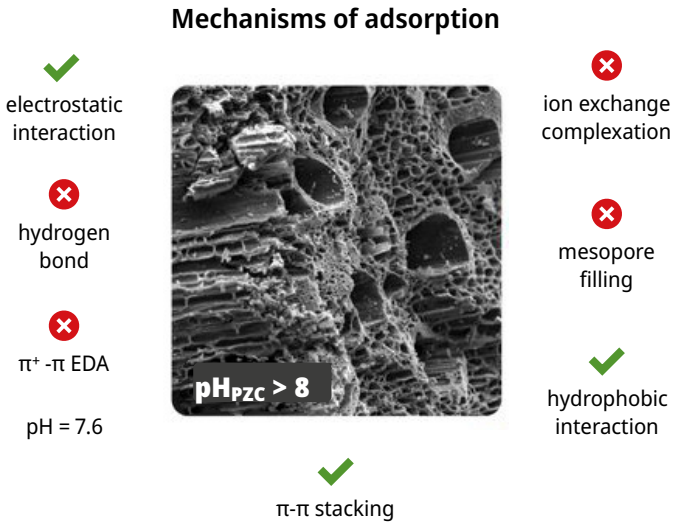

FIGURE 3. List of potential MCLR adsorption mechanisms on carbonaceous materials, with the green ticks outlining those elucidated for bamboo biochar 600B0.5.

TABLE 4. MCLR adsorption capacity of various carbonaceous materials and the mainly proposed mechanism.

Materials	Adsorption capacity	Mechanism	Reference
Wood-based AC	189 μg mg^{-1}	Pore –filling (secondary micropores and mesopores)	(Pendleton et al., 2001)
Rice straw-derived biochar	10.96 μg g^{-1}	Electrostatic interactions and Hydrogen bonds	(Wei and Lu, 2021)
Chicken manure-derived biochar	>1050 μg g^{-1}	Electrostatic interaction related to higher ash content at low pH	(Li et al., 2018)
Bamboo/chitosan-derived biochar	1 mg g^{-1}	Ion pairing effect at low pH	(Zhang et al., 2011)
Mesoporous carbon	37.87 mg g^{-1}	(meso-)pore diffusion and π – π (and hydrophobic) interactions	(Park et al., 2020)
Graphene oxide	1700 μg g^{-1}	Ion-pairing effect at low pH	(Pavagadhi et al., 2013)
Giant reed-derived biochar	42.4 mg g^{-1}	Hydrophobic interaction and $π^+$-π or π-π interaction	(Liu et al., 2018)
Nanotubes	14.8 mg g^{-1}	Nanotubes 10nm filling	(Yan et al., 2006)
Bamboo biochar	200 μg g^{-1}	Electrostatic interaction, hydrophobic interaction and π-π interaction	This work

CONCLUSIONS

Bamboo biochars were systematically synthesized, varying the pyrolysis temperatures and residence times. The influence of time on the surface chemistry and textural characteristics of the biochars is minimal compared to the impact of temperature. Among bamboo biochars, sample 600B0.5 exhibits a remarkable combination of well-developed macroporous structures, an optimal aromatization degree, and a basic nature, resulting in efficient and effective removal of MCLR: 91 % in batch (Q_{max} = 219 μg g^{-1}) at a pH of 7.63 comparable to that in water treatment plants and, 99.5 % in column, resulting in a final concentration of 0.28 μg L^{-1}, well below the World Health Organization guideline of 1 μg L^{-1} (World Health Organization, 2020). The MCLR uptake mechanism under this condition was mainly determined by electrostatic, π-π stacking, and hydrophobic interactions.

ACKNOWLEDGEMENTS

Authors acknowledge Bambú del Este for the biomass supply, Laboratorio de Sólidos Porosos, Universidad Nacional de San Luis (Argentina) for the nitrogen isotherms, thermogravimetric analysis and mercury porosimetry, Ricardo Faccio for Raman measurements. This work was supported by the Centro Tecnológico del Agua [CGA2020-06].

REFERENCES

American Society for Testing and Materials, 2021. D3172-13, reapproved 2021: *Proximate analysis of coal and coke*. West Conshohocken: ASTM.

Carmichael, W. W. and Boyer, G. L., 2016. Health impacts from cyanobacteria harmful algae blooms: implications for the North American great lakes. In: *Harmful Algae,* 54*,* pp. 194–212. DOI: https://doi.org/10.1016/J.HAL.2016.02.002

Chaturvedi, K.; Singhwane, A.; Dhangar, M.; Mili, M.; Gorhae, N.; Naik, A.; Prashant, N.; Srivastava, A. K. and Verma, S., 2023. Bamboo for producing charcoal and biochar for versatile applications. En: *Biomass Conv. Bioref.* DOI: https://doi.org/10.1007/s13399-022-03715-3

Chen, B. and Chen, Z., 2009. Sorption of naphthalene and 1-naphthol by biochars of orange peels with different pyrolytic temperatures. In: *Chemosphere*, 76(1), pp. 127–133. DOI: https://doi.org/10.1016/j.chemosphere.2009.02.004

El Bouaidi, W.; Enaime, G.; Loudiki, M.; Yaacoubi, A.; Douma, M.; Ounas, A. and Lübken, M., 2022. Adsorbents used for microcystin removal from water sources: current knowledge and future prospects. In: *Processes*, 10(7), pp. 1–23. DOI: https://doi.org/10.3390/pr10071235

Fries, M. and Steele, A., 2010. Raman spectroscopy and confocal Raman imaging in mineralogy and petrography. In: *Springer Series in Optical Sciences*, 158, pp. 111–135. DOI: https://doi.org/10.1007/978-3-642-12522-5_6/

Frišták, V.; Laughinghouse, H. D. and Bell, S. M., 2020. The use of biochar and pyrolysed materials to improve water quality through microcystin sorption separation. In: *Water (Switzerland)*, 12(10), pp. 1–19. DOI: https://doi.org/10.3390/w12102871

Li, J.; Cao, L.; Yuan, Y.; Wang, R.; Wen, Y. and Man, J., 2018. Comparative study for microcystin-LR sorption onto biochars produced from various plant- and animal-wastes at different pyrolysis temperatures: Influencing mechanisms of biochar properties. In: *Bioresource Technology*, 247(July 2017), pp. 794–803. DOI: https://doi.org/10.1016/j.biortech.2017.09.120

Li, L.; Qiu, Y.; Huang, J.; Li, F. and Sheng, G. D., 2014. Mechanisms and factors influencing adsorption of Microcystin-LR on biochars. In: *Water, Air, and Soil Pollution*, 225(12). DOI: https://doi.org/10.1007/s11270-014-2220-6

Liu, G.; Zheng, H.; Zhai, X. and Wang, Z., 2018. Characteristics and mechanisms of microcystin-LR adsorption by giant reed-derived biochars: Role of minerals, pores, and functional groups. En: *Journal of Cleaner Production*, 176, pp. 463–473. DOI: https://doi.org/10.1016/j.jclepro.2017.12.156

Manals-Cutiño, E.; Penedo-Medina, M. and Giralt-Ortega, G., 2011. Análisis termogravimétrico y térmico diferencial de diferentes biomasas vegetales [Online]. In: *Tecnología Química*, XXXI(2), pp. 36–43. [Accessed: 12 april 2024]. Retrieved from: https://www.redalyc.org/articulo.oa?id=445543773005

Melaram, R.; Newton, A. R. and Chafin, J., 2022. Microcystin contamination and toxicity: implications for agriculture and public health. In: *Toxins*, 14(5). DOI: https://doi.org/10.3390/TOXINS14050350

Odoemelam, S.; Onwu, F.; Uchechukwu, S. and Chinedu, M., 2015. Adsorption Isotherm Studies of Cd(ll) and Pb(ll) Ions from Aqueous Solutions by Bamboo-Based Activated Charcoal and Bamboo Dust. In: *American Chemical Science Journal*, 5(3), pp. 253–269. DOI: https://doi.org/10.9734/acsj/2015/14425

Park, J. A.; Kang, J. K.; Jung, S. M.; Choi, J. W.; Lee, S. H.; Yargeau, V. and Kim, S. B., 2020. Investigating Microcystin-LR adsorption mechanisms on mesoporous carbon, mesoporous silica, and their amino-functionalized form: Surface chemistry, pore structures, and molecular characteristics. In: *Chemosphere*, 247, 125811. DOI: https://doi.org/10.1016/j.chemosphere.2020.125811

Pavagadhi, S.; Tang, A. L. L.; Sathishkumar, M.; Loh, K. P. and Balasubramanian, R., 2013. Removal of microcystin-LR and microcystin-RR by graphene oxide: Adsorption and kinetic experiments. In: *Water Research*, 47(13), pp. 4621–4629. DOI: https://doi.org/10.1016/j.watres.2013.04.033

Pendleton, P.; Schumann, R. and Wong, S. H., 2001. Microcystin-LR Adsorption by activated carbon. In: *Journal of Colloid and Interface Science*, 240(1), pp. 1–8. DOI: https://doi.org/10.1006/JCIS.2001.7616

Ren, X.; Wang, Y.; Zhang, K.; Ding, Y.; Zhang, W.; Wu, M.; Xiao, B. and Gu, P., 2023. Transmission of microcystins in natural systems and resource processes: a review of potential risks to humans health. In: *Toxins*, 15(7). DOI: https://doi.org/10.3390/toxins15070448

Rouquerol, J.; Llewellyn, P. and Rouquerol, F., 2007. Is the bet equation applicable to microporous adsorbents? In: *Studies in Surface Science and Catalysis*, 160, pp. 49–56. DOI: https://doi.org/10.1016/S0167-2991(07)80008-5

Teng, W.; Wu, Z.; Fan, J.; Chen, H.; Feng, D.; Lv, Y.; Wang, J.; Asiri, A. M. and Zhao, D., 2013a. Ordered mesoporous carbons and their corresponding column for highly efficient removal of microcystin-LR. In: *Energy and Environmental Science*, 6(9), pp. 2765–2776. DOI: https://doi.org/10.1039/c3ee41775a

Teng, W.; Wu, Z.; Feng, D.; Fan, J.; Wang, J.; Wei, H.; Song, M. and Zhao, D., 2013b. Rapid and efficient removal of microcystins by ordered mesoporous silica. In: *Environmental Science and Technology*, 47(15), pp. 8633–8641. DOI: https://doi.org/10.1021/es400659b

Thommes, M.; Kaneko, K.; Neimark, A. V.; Olivier, J. P.; Rodriguez-Reinoso, F.; Rouquerol, J. and Sing, K. S. W., 2015. Physisorption of gases, with special reference to the evaluation of surface area and pore size distribution (IUPAC Technical Report). In: *Pure and Applied Chemistry*, 87(9–10), pp. 1051–1069. DOI: https://doi.org/10.1515/pac-2014-1117

Uruguay. Agencia Reguladora de Compras Estatales, 2022. *Licitación abreviada 23041/2022* [Online]. Montevideo: Administración de las Obras Sanitarias del Estado. [Accessed: 24 april 2024]. Available at: https://www.comprasestatales.gub.uy/consultas/detalle/id/i366680

Uruguay. Ministerio de Vivienda Ordenamiento Territorial y Medioambiente, 2020. *Informe, evolución de la calidad del agua en la cuenca del Río Santa Lucía* [Online]. Montevideo: DINAMA. [Accessed: 12 april 2024]. Available at: https://www.gub.uy/ministerio-ambiente/sites/ministerio-ambiente/files/documentos/publicaciones/Informe-Santa-Lucia-2015-2019.pdf

Verma, S.; Kumar, P.; and Lavrenčič Štangar, U., 2023. A Perspective on removal of cyanotoxins from water through advanced oxidation processes. In: *Global Challenges*, 2300125, pp. 1–11. DOI: https://doi.org/10.1002/gch2.202300125

Wei, L. and Lu, J., 2021. Adsorption of microcystin-LR by rice straw biochars with different pyrolysis temperatures. In: *Environmental Technology and Innovation*, 23, 101609. DOI: https://doi.org/10.1016/j.eti.2021.101609

World Health Organization, 2020. *Cyanobacterial toxins: microcystins. Background document for development of WHO Guidelines for drinking-water quality and Guidelines for safe recreational water environments* [Online]. Ginebra: WHO. [Accessed: 24 april 2024]. Available at: https://apps.who.int/iris/handle/10665/338066

Yan, H.; Gong, A.; He, H.; Zhou, J.; Wei, Y. and Lv, L., 2006. Adsorption of microcystins by carbon nanotubes. In: *Chemosphere*, 62(1), pp. 142–148. DOI: https://doi.org/10.1016/j.chemosphere.2005.03.075

Zegura, B., 2016. An overview of the mechanisms of Microcystin-LR genotoxicity and potential carcinogenicity. In: *Mini-Reviews in Medicinal Chemistry*, 16(13), pp. 1042–1062. DOI: https://doi.org/10.2174/1389557516666160308141549

Zhang, H.; Zhu, G.; Jia, X.; Ding, Y.; Zhang, M.; Gao, Q.; Ciming, H. and Xu, S., 2011. Removal of microcystin-LR from drinking water using a bamboo-based charcoal adsorbent modified with chitosan. In: *Journal of Environmental Sciences*, 23(12), pp. 1983–1988. DOI: https://doi.org/10.1016/S1001-0742(10)60676-6

ANNEXES

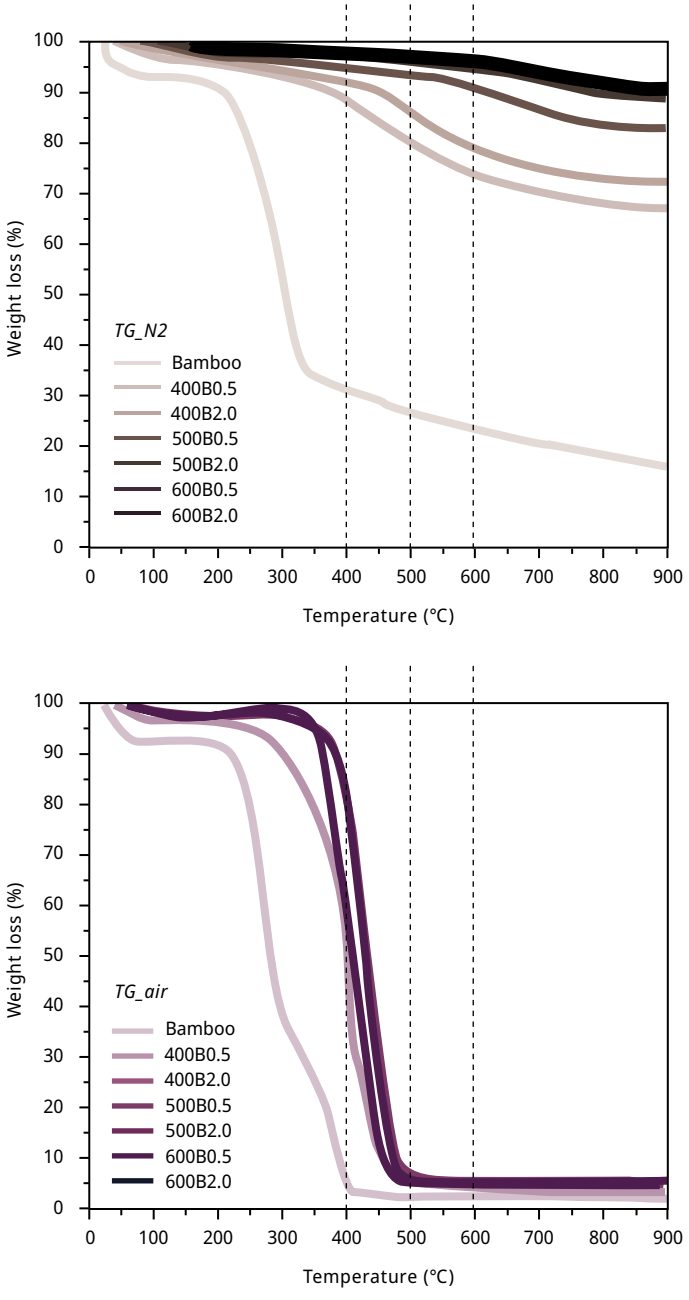

FIGURE A1. Thermogravimetric analysis (TG) for bamboo and bamboo biochars performed at heating rates of 10 °C min^{-1} with temperatures ranging from room temperature to 900 °C. Compressed air (left) and nitrogen (right) was used for combustion experiments at 50 mL min^{-1}.

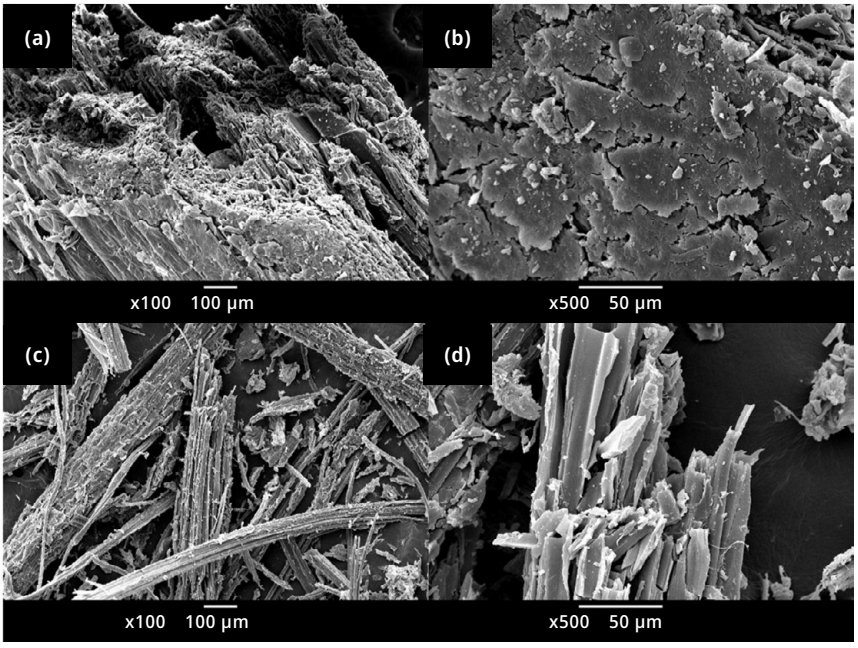

FIGURE A2. Scanning electron microscopic images of (a) bamboo biomass x100, and (b) bamboo biomass x500, and (c) 500B2.0 x100 and (d) 500B2.0 x500.

TABLE A1. Raman shifts of the D and G bands observed in the six bamboo biochars, along with the intensity ratio I_D/I_G.

	D band	G band	
Sample	Raman Shift	Raman Shift	Ra, I_D/I_G
400B0.5	1352.5	1568.3	2.37
400B2.0	1354.1	1568.2	2.46
500B0.5	1343.7	1566.9	2.24
500B2.0	1346.4	1568.7	2.18
600B0.5	1340.0	1568.3	2.08
600B2.0	1340.1	1568.2	2.05

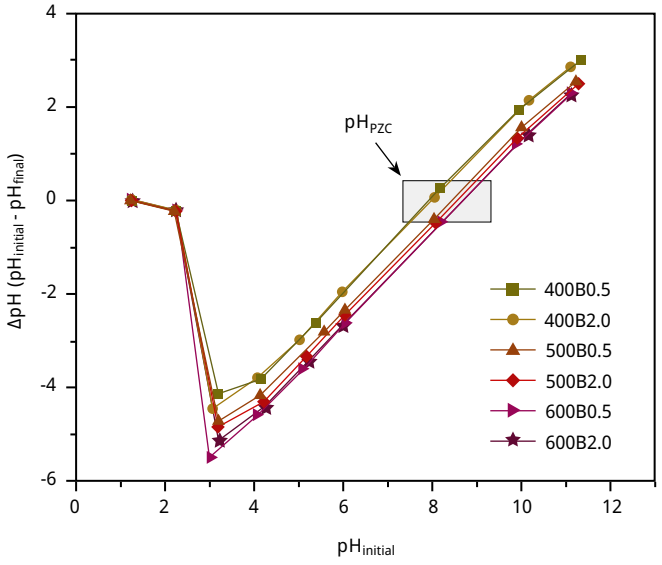

FIGURE A3. Plot of ΔpH vs. initial pH for $pH_{PZC's}$ determination of the six bamboo biochars.

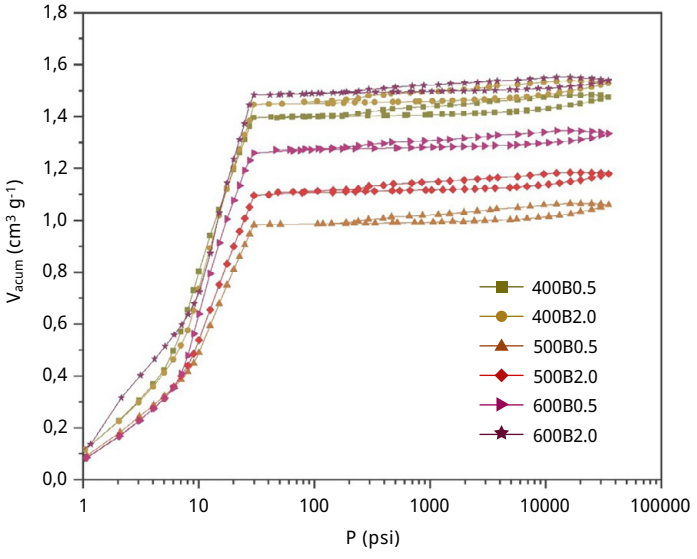

FIGURE A4. Hg intrusion-extrusion curves for the six bamboo biochars.

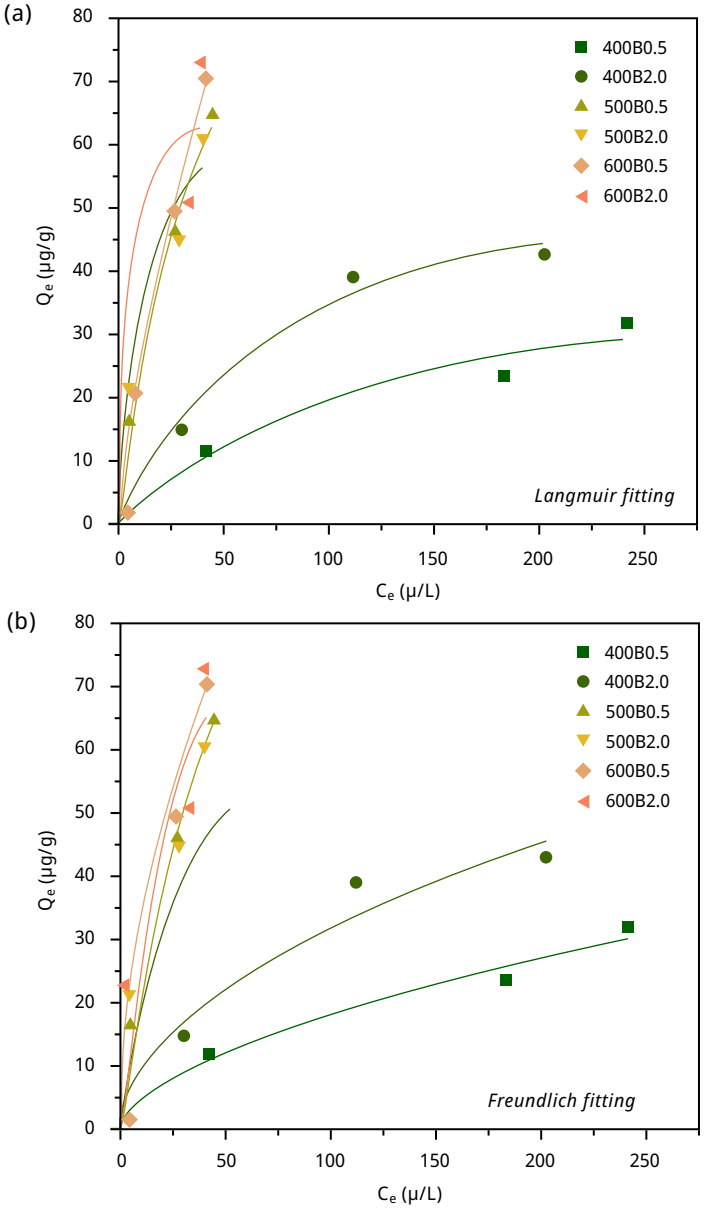

FIGURE A5. Adsorption isotherm of MCLR (scatters) on the six bamboo biochars with (a) Langmuir model fitting (lines), (b) Freundlich model fitting (lines).

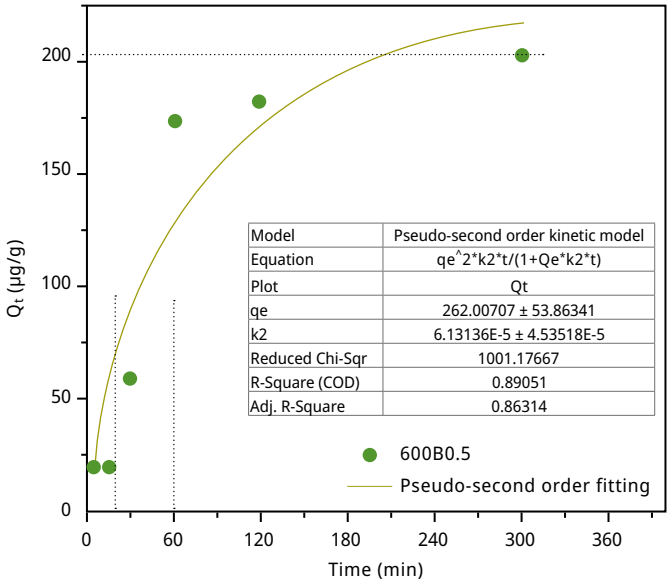

FIGURE A6. Adsorption capacity at the time t (Q_t) versus contact time on the sample 600B0.5 with an initial concentration of 500 µg L^{-1} in water.

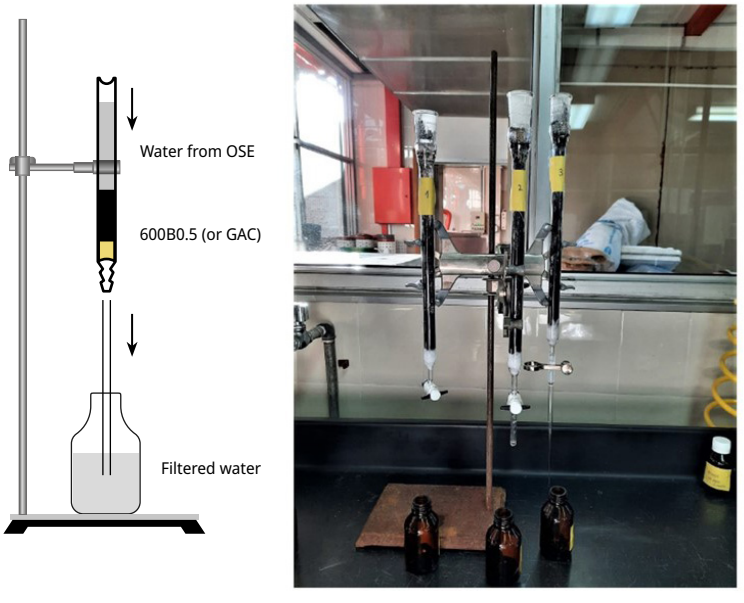

FIGURE A7. Scheme of the setup (left). Photograph of the column built in the (right). OSE refers to National Administration of State Sanitary Works.

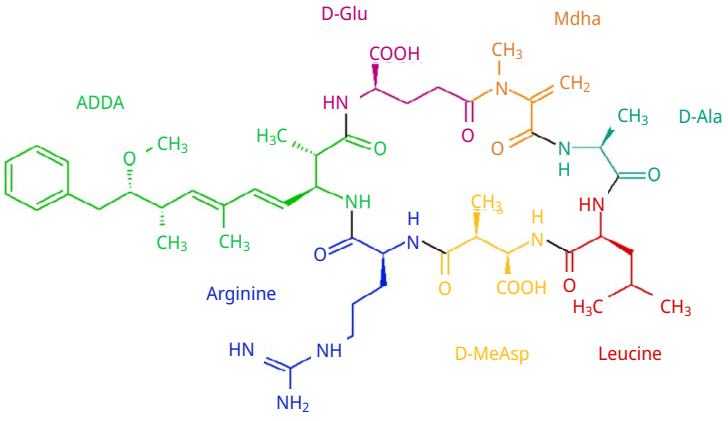

FIGURE A8. MCLR chemical structure.